

## Coil-to-stretch transition, kink formation, and efficient barrier crossing of a flexible chain

SeungKyun Lee and Wokyung Sung

Department of Physics and Institute of Polymer Research, Pohang University of Science and Technology, Pohang 790-784, South Korea

(Received 14 June 2000; published 26 January 2001)

We study the thermally activated barrier crossing of a linear, flexible chain (polymer) under the Kramers bistable potential using the multidimensional barrier crossing theory and the functional integral method. We find that above a critical chain length or below a critical chain spring constant the chain at the barrier top undergoes coil-to-stretch transition, resulting in the formation of a kink. The emergence of the kink mode renormalizes the activation energy to a smaller value so as to facilitate the barrier crossing. In addition to this, the larger fluctuation of the polymer in the unstable region of the potential (compared to that in the confining well) further reduces the free energy barrier, and greatly enhances the crossing rate of a flexible chain. We calculate analytically the crossing rates and confirm the results by numerical simulations. The polymer in barrier crossing thus reveals its conformational flexibility and adjustment to external forces as characteristic features of soft matter dynamics.

DOI: 10.1103/PhysRevE.63.021115

PACS number(s): 05.40.-a, 61.41.+e, 82.20.Db, 87.15.He

## I. INTRODUCTION

The thermally activated barrier crossing is not only of fundamental importance in describing many practical problems in physics, chemistry, and biology, but also instrumental in understanding stochastic paradigms such as stochastic resonance and thermal ratchets, which have attracted much attention recently [1]. Since Kramers treatment of the barrier crossing dynamics of a Brownian particle interacting with the environment, much progress has been made in this field [2] to study the barrier crossing rate of a single particle (or degree of freedom) in various complex situations including those with memory effect [3], nonequilibrium fluctuation [4], and quantum tunneling [5]. Recently, on the other hand, there has been much interest in the stochastic dynamics of systems consisting of more than one degree of freedom. An outstanding example is the array-enhanced stochastic resonance [6]. There, the optimal signal-to-noise ratio of the response of a typical element in an array of periodically forced, damped bistable oscillators is greatly enhanced when suitable coupling is introduced between neighboring oscillators. Other examples include the synchronization-like behavior of two coupled stochastic bistable systems [7] and directed transport of two or more elastically coupled particles in a ratchet potential under nonequilibrium fluctuation [8,9]. A main concern in these examples has been the effect of the coupling on the coherent dynamics of the whole system.

As interconnected, flexible systems as they are, polymers and membranes manifest interesting cooperative dynamics of biological relevance in certain noisy environments and external fields. In particular, the transport of polymers in inhomogeneous media has been widely studied with possible applications to DNA/RNA manipulation, drug delivery, and protein inclusion and penetration through cell membranes. In recent years, the translocation of a long flexible polymer through a membrane pore has been a subject of active investigation, where it is important to understand the driving and blocking mechanisms [10,11]. Slater *et al.* suggested an interesting ‘‘entropic ratchet’’ mechanism for a polymer moving in a channel with an asymmetrically modulated cross

section [12]. Diffusion of polymers in random porous media has also been much studied in connection with gel electrophoresis [13]. Han *et al.* have reported a controlled experiment on the escape of a long trapped DNA chain through a narrow pathway [14]. These studies showed that the entropic effect coming from the conformational flexibility of polymers plays an important role in determining their dynamical properties, and revealed some remarkable effects of chain connectivity in the presence of external fields and environmental biases.

In this paper, we consider a thermally activated barrier crossing or the escape of a linear flexible chain (polymer) over the barrier of a Kramers bistable potential (Fig. 1). With the chain being viewed as a coupled array of  $N$  Brownian particles (beads), each subject to the potential, the problem is a generalization of the well known Kramers theory to many degrees of freedom. Although for a real polymer under an unstable potential, anharmonic segmental tension can be invoked for finite chain extensibility, here we only consider a chain with simple harmonic coupling between neighboring beads (Rouse model). Our model will be appropriate for a situation where the barrier curvature is small on microscopic scales so that the extension of individual segments remains

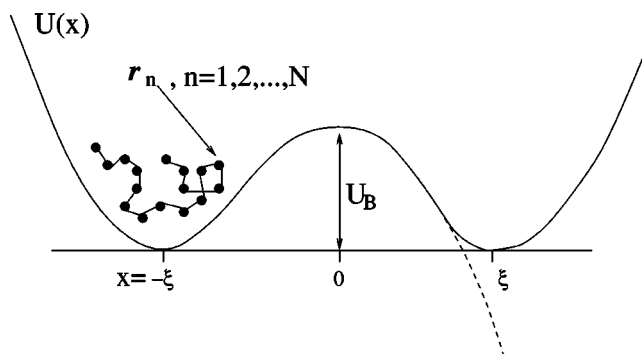


FIG. 1. A linear chain of  $N$  identical beads under bistable potential  $U(x)$ . The potential has local wells at  $x = \pm \xi$  and a barrier at  $x = 0$ . The dashed line indicates the metastable Kramers potential considered in [15].

small throughout the dynamics of the chain. In a related study, Park and Sung [15] considered a metastable Kramers potential varying on a length scale much larger than the polymer size, with one side falling to negative infinity (dashed line, Fig. 1). There, a chain with harmonic coupling can extend indefinitely at the barrier top when  $N$  is sufficiently large. Therefore, to overcome the difficulty, a lattice polymer model was used for numerical computations [15].

Recently, Sebastian and Paul [16] considered a similar problem of barrier crossing of a polymer in a double-well potential in the opposite case, with the barrier width much smaller than the polymer contour length. In their solution, part of the polymer is first activated over the barrier to form a kink or a kink/antikink pair (hairpin), and then the entire polymer translocates to the other side of the barrier by movement of the kink (and/or antikink) along the contour. Because the kink or antikink is essentially a localized object in the long-chain limit, the activation energy is independent of the chain length, and the crossing rates for polymers of different lengths are determined by the kink diffusion time along the chain.

Motivated by polymer transport in mesoscopically or macroscopically modulating environments, we will consider a Kramers potential with a barrier of large enough width that the barrier crossing process is dominated by the activation of the entire polymer over the barrier top, rather than by the motion of a preformed, localized kink. In this case, the activation energy depends critically on the number of monomers  $N$ . In the short chain limit, the polymer will maintain its free-space configuration of coiled form, since the potential does not vary significantly over its radius of gyration. Thus the activation energy is proportional to  $N$ , and the crossing is slowed down exponentially as  $N$  grows. But this cannot go on indefinitely as we increase  $N$  because at some point the polymer is capable of undergoing conformational transition to a stretched state to greatly lower the activation energy. Upon further increase of  $N$ , the mode of translocation will eventually become that of kink diffusion as considered in [16].

Our aim in this paper is to describe analytically the onset of this coil-to-stretch transition and its effect on the free-energy barrier as well as the crossing rate. It is found that beyond the transition, which can be tuned either by the length of the polymer or the coupling strength, the first Rouse mode gives rise to the kink formation, which lowers the free-energy barrier to enhance the crossing rate. Also, the large fluctuation occurring near the transition point is found to contribute significantly to the reduction of free-energy barrier.

In Sec. II we define our model and the problem more precisely. Using the functional integral method for evaluating the free energy, we calculate the chain crossing rate for a bistable potential and harmonic coupling in Sec. III. The main theoretical base is the multidimensional Kramers rate theory applied to the dynamics in chain configuration space. Analytical expressions of the rate are obtained in ranges of potential and chain parameters which cannot only be relevant to polymer transport in potentials varying on mesoscopic or macroscopic scales, but also show dominant effects of chain

flexibility and the associated conformational transition that we seek to find in this work. Results of our numerical simulations are presented in Sec. IV, and Sec. V summarizes the paper.

## II. DEFINITION OF THE PROBLEM AND MULTIDIMENSIONAL KRAMERS RATE THEORY

Consider a linear chain of  $N$  identical beads in three-dimensional (3D) space which is initially confined in one well of a one-dimensional bistable potential  $U(x) = -(\omega_B^2/2)x^2 + 1/4(\omega_B^2/\xi^2)x^4$  (Fig. 1). The potential  $U(x)$  has two local wells at  $x = \pm \xi$  separated by a barrier centered at  $x = 0$ . The barrier has the height  $U_B = U(0) - U(\pm \xi) = \omega_B^2 \xi^2/4$  and the width  $2\xi$ . The  $\omega_B^2$  and  $\omega_0^2 \equiv 2\omega_B^2$  are the curvatures at potential maximum and minimum. Our question is: what is the rate or inverse mean time of the thermally activated crossing of the whole chain from one well to the other? To simplify the problem, we confine ourselves to the case where the crossing dynamics is much slower than the internal chain relaxation so that multidimensional Kramers theory is valid as described below. For the interaction between the beads, we consider only the nearest neighbor coupling characterized by the potential  $V(\Delta r) = V(|\mathbf{r}_{n+1} - \mathbf{r}_n|)$ ,  $n = 1, 2, \dots, N-1$ , where  $\mathbf{r}_n$ ,  $n = 1, 2, \dots, N$  denotes the position of the  $n$ th bead. For simplicity, we neglect other inter-bead interactions that give rise to excluded volume effect and bending stiffness.

In many cases, the simple bead spring model for the chain,  $V(\Delta r) = \frac{1}{2}K(\Delta r)^2$ ,  $K = 3k_B T/l^2$  where  $l$  is the mean free-space segmental length, gives a satisfactory description of the conformation and dynamics of a real polymer. Strictly speaking, the segmental tension of a real polymer in the presence of an external potential becomes nonlinear [i.e., anharmonic terms in  $V(\Delta r)$  become important] when the segmental length exceeds some tolerance range, say  $\zeta$ . When the potential has a barrier of width  $2\xi$  and a curvature at the top given by  $\omega_B^2$ , we can show that in thermal equilibrium the segment of a harmonic chain will be extended at most by  $\Delta x \sim \xi \sqrt{\omega_B^2/K}$  [17] in the direction of potential variation. Hence we get the following self-consistent condition for the harmonic description of the coupling function:

$$\zeta \gtrsim \xi \sqrt{\frac{\omega_B^2}{K}} \quad (1)$$

where  $\zeta$  is a chain parameter describing the range of segmental extension beyond which the Hooke's law breaks down. We may assume in good approximation that the chain in free space is harmonic, that is,  $\zeta$  is sufficiently larger than the free-space mean segmental length,  $\zeta > \sqrt{k_B T/K}$ . Then the above condition is guaranteed if  $k_B T \gtrsim \omega_B^2 \xi^2$ , which means that the barrier height is, at most, of the order of  $k_B T$  per segment. In what follows, we consider the parameter regime where Eq. (1) is met, thus neglecting anharmonic terms in  $V(\Delta r)$ ;  $V(\Delta r) = \frac{1}{2}K(\Delta r)^2$ .

Now the total energy of the chain under potential  $U(x)$  is

$$\Phi(\{\mathbf{r}_n\}) = \sum_{n=1}^N U(x_n) + \sum_{n=1}^{N-1} \frac{1}{2} K |\mathbf{r}_{n+1} - \mathbf{r}_n|^2.$$

If we work in the overdamped limit where the bead's momentum relaxation has occurred already in the relevant time scale, we can regard the escape process as a Brownian motion occurring in the  $3N$ -dimensional configuration space of the chain where the above energy function is defined. Noting that the energy function does not involve coupling between different Cartesian coordinates of  $\{\mathbf{r}_n\} = \{x_n, y_n, z_n\}$ , we can reduce the problem further by separating the dynamics along the  $x$  direction governed by the energy function

$$\Phi(\{x_n\}) = \sum_{n=1}^N U(x_n) + \sum_{n=1}^{N-1} \frac{1}{2} K (x_{n+1} - x_n)^2. \quad (2)$$

The probability distribution  $P(\{x_n\}; t)$ , which represents the probability per unit volume (in  $\{x_n\}$  space) of the chain to have configuration  $\{x_n\}$  at time  $t$ , satisfies the following Fokker-Planck equation:

$$\frac{\partial P(\{x_n\}; t)}{\partial t} = D \sum_l \frac{\partial}{\partial x_l} \left[ \frac{\partial}{\partial x_l} + \beta \frac{\partial}{\partial x_l} \Phi(\{x_n\}) \right] P(\{x_n\}; t), \quad (3)$$

where  $D$  is the segmental diffusion coefficient and  $\beta = (k_B T)^{-1}$ . In the  $y$  and  $z$  directions the chain simply shows the free-space Rouse chain dynamics.

The configuration space  $\{x_n\}$  contains two stable points that correspond to the chains localized at  $x = +\xi$  or  $x = -\xi$ . These two states, which we will denote by  $\{\bar{x}_n\}_+$  and  $\{\bar{x}_n\}_-$ , are separated by a higher-energy region or barrier in  $\{x_n\}$  space. Our problem is to find the rate at which our system (chain) starts from its initial confinement around  $\{\bar{x}_n\}_-$  and escapes over the barrier to reach the well around  $\{\bar{x}_n\}_+$ . The relevant activation energy of this process is the lowest threshold energy in all the paths connecting the states  $\{\bar{x}_n\}_-$  and  $\{\bar{x}_n\}_+$ . Geometrically, it is determined by the path crossing the saddle point  $\{\bar{x}_n\}_B$  in the configuration space, which is a stationary point with respect to a variation ( $\delta$ ) satisfying

$$\delta \Phi|_{\{\bar{x}_n\}_B} = 0$$

and involving only one unstable mode along which the ‘‘reaction flux’’ runs from  $\{\bar{x}_n\}_-$  to  $\{\bar{x}_n\}_+$ . In the next section we will see that this ‘‘transition state’’  $\{\bar{x}_n\}_B$  corresponds to either a localized configuration of  $\{x_n\}$  around  $x=0$ , or a kink configuration representing a stretched chain around  $x=0$ , depending on the chain and potential parameters.

In any case, let us denote the activation energy as  $\Delta\Phi = \Phi(\{\bar{x}_n\}_B) - \Phi(\{\bar{x}_n\}_-)$ . If  $\Delta\Phi \gg k_B T$ , the crossing time is much longer than any internal chain relaxation time, and it can be calculated from an approximate, quasistationary solution to Eq. (3). The rate is obtained by dividing the reaction flux  $j$  across the saddle point  $\{\bar{x}_n\}_B$  by the total probability

population confined in the well at  $\{\bar{x}_n\}_-$ . This is the famous Kramers rate theory in the overdamped limit formulated by Langer [18]. The resulting rate  $\mathcal{R}$  is written as

$$\mathcal{R} = \frac{\omega_B}{2\pi\gamma} \frac{Z_B}{Z_0} \sqrt{2\pi k_B T} e^{-\beta\Delta\Phi}. \quad (4)$$

$Z_0$  and  $Z_B$  are, respectively, the partition functions associated with the fluctuation of the system near the initial stable point  $\{\bar{x}_n\}_-$  and near the saddle point  $\{\bar{x}_n\}_B$ . Explicitly,

$$Z_0 = \int_{\text{well}} d^N \{x_n\} e^{-\beta[\Phi(\{x_n\}) - \Phi(\{\bar{x}_n\}_-)]}, \quad (5)$$

$$Z_B = \int_{\perp(\text{unstable mode})}^{\text{saddle}} d^{N-1} \{x_n\} e^{-\beta[\Phi(\{x_n\}) - \Phi(\{\bar{x}_n\}_B)]}. \quad (6)$$

The integral in Eq. (6) is over the hypersurface which contains the saddle point and is normal to the unstable mode. The rate equation (4) can also be written as

$$\mathcal{R} = \frac{\omega_0 \omega_B}{2\pi\gamma} e^{-\beta\Delta F}, \quad (7)$$

where  $\Delta F$  is the free-energy barrier defined by

$$\Delta F \equiv \Delta\Phi - k_B T \ln(Z_B/Z'_0), \quad (8)$$

where  $Z'_0$  is the partition function at the well with the lowest-mode contribution omitted;  $Z'_0 \equiv Z_0 / (\sqrt{2\pi k_B T} \omega_0^{-1})$ .  $\Delta F$  consists of both the activation energy  $\Delta\Phi$  and the difference in the free energy of fluctuation around  $\{\bar{x}_n\}_B$  and  $\{\bar{x}_n\}_-$ .

Note that the above rate formalism can be applied to our problem if we identify a well defined transition state of the chain represented by a localized saddle point in the configuration space. This can be seen by noting that the expression Eq. (4) gives the rate in terms of only local properties of the saddle and the metastable points, without showing dependence on, for example, the distance between these points in  $\{x_n\}$  space. One example with such dependence is when the chain contour length is much larger than the width of the barrier so that the chain translocation from one well to the other occurs via movement along the chain contour of an extended portion (kink) of the chain bridging the two wells, while the remaining majority of segments reside in one well or another [16]. In the following sections, we will concentrate on the case of a relatively wide barrier and a small chain for which the rate expression Eq. (4) obtained by the multi-dimensional Kramers theory is valid.

### III. CALCULATION OF THE RATE

Consider the quartic double-well potential  $U(x)$  in Fig. 1. If the number of beads  $N$  is large and the attractive coupling among the beads is strong so that any two neighboring beads always remain close to each other in the length scale over which  $U(x)$  varies, we can treat the  $N$ -bead chain as a continuous string represented by a path,  $\{x_n\} \rightarrow \{x(s=s/N)\}$ ,  $0 \leq s \leq 1$ . In this limit, via transformation  $\sum_{n=1}^N \rightarrow N \int_0^1 ds$  and

$|x_{n+1} - x_n| \rightarrow \frac{1}{N} |\dot{x}(s)|$ , we get the energy functional

$$\Phi = \Phi[x(s)] = N \int_0^1 ds \mathcal{L}[x(s), \dot{x}(s)], \quad (9)$$

$$\mathcal{L}[x(s), \dot{x}(s)] = -\frac{\omega_B^2}{2} x(s)^2 + \frac{1}{4} \frac{\omega_B^2}{\xi^2} x(s)^4 + \frac{1}{2} \frac{K}{N^2} \dot{x}(s)^2,$$

where  $\dot{x} \equiv dx/ds$ . The free-end boundary condition, consistent with the bead-spring model [19], is expressed as  $dx/ds = 0$  at  $s=0,1$ . In order to perform the functional integration for the partition functions [Eqs. (5,6)], we need to identify the stationary solution to Eq. (9) around which the fluctuation is to be evaluated.

The stationary path(s) is(are) obtained from the Euler-Lagrange equation [20]

$$\frac{\partial \mathcal{L}}{\partial x} = \frac{d}{ds} \frac{\partial \mathcal{L}}{\partial \dot{x}}, \quad 0 < s < 1,$$

which yields the differential equation for the stationary path  $\bar{x}(s)$ ,

$$\frac{K}{N^2} \ddot{\bar{x}}(s) = -\omega_B^2 \bar{x} + \frac{\omega_B^2}{\xi^2} \bar{x}^3, \quad 0 < s < 1, \quad (10)$$

with boundary condition  $\dot{\bar{x}}(0) = \dot{\bar{x}}(1) = 0$ .  $\bar{x}(s)$  can be regarded as the trajectory of a classical particle moving in the inverted potential  $-U(x)$ , with zero initial and final ‘‘velocities.’’

There are three trivial solutions consistent with the boundary condition:

$$\bar{x}(s) \equiv 0, \pm \xi. \quad (11)$$

It is obvious that the solutions  $\bar{x}(s) \equiv \pm \xi$ , corresponding to the chains confined in either well, are stable. We will assume that the chain is initially confined in the left well near  $x = -\xi$ , so that the metastable configuration is denoted by  $\bar{x}_0(s) = \bar{x}_-(s) \equiv -\xi$ . We can show that Eq. (11) is the only solution when  $N^2 \omega_B^2 < K \pi^2$ . Thus in this parameter regime the homogeneous configuration  $\bar{x}(s) \equiv 0$  is the only saddle point (in  $\{x_n\}$  space) bridging the two stable states  $\bar{x}(s) \equiv \pm \xi$ . We will denote such transition state  $\bar{x}_B(s)$ .

To assess the effects of the fluctuation and the saddle point structure of the chain energy functional we investigate the eigenvalue spectrum of the operator of second-order expansion of  $\Phi$  at the stationary points. This operator is defined by the expansion

$$\Phi[\bar{x} + \delta x] = \Phi[\bar{x}] + \frac{N}{2} \int_0^1 ds \delta x(s) \Phi \delta x(s) + \mathcal{O}[(\delta x)^4], \quad (12)$$

and corresponds to the differential operator

$$\Phi \leftrightarrow U''[\bar{x}(s)] - \frac{K}{N^2} \frac{d^2}{ds^2} \quad (13)$$

defined in the function space  $\{u(s), 0 \leq s \leq 1, \dot{u}(0) = \dot{u}(1) = 0\}$ . The operator  $-(K/N^2)(d^2/ds^2)$  has the eigenvalue spectrum  $(K/N^2)\pi^2 j^2$ ,  $j=0,1,\dots,N-1$ , associated with the eigenfunctions (normalized to unity) known as the Rouse modes,

$$u_j(s) = \begin{cases} \sqrt{2} & j=1,2,\dots,N-1 \\ 1 & j=0 \end{cases} \cos(\pi j s).$$

Hence at  $\bar{x}_0(s) \equiv -\xi$ ,  $\Phi$  has the eigenvalues  $\lambda_j^0 = U''(-\xi) + (K/N^2)\pi^2 j^2$ ,  $j=0,1,\dots,N-1$ , which are all positive, confirming that these solutions correspond to stable configurations. Note that  $U''(-\xi) = 2\omega_B^2 = \omega_0^2$ . At  $\bar{x}_B(s) \equiv 0$ , the eigenvalues of  $\Phi$  are  $\lambda_j^B = -\omega_B^2 + (K/N^2)\pi^2 j^2$ ,  $j=0,1,\dots,N-1$ . Here the smallest eigenvalue is negative ( $= -\omega_B^2$ ). The next eigenvalue, associated with the first Rouse mode  $u_1(s) = \sqrt{2} \cos(\pi s)$ , is positive as long as

$$\omega_B^2 < \frac{K \pi^2}{N^2} \quad (14)$$

(coiled-state barrier crossing regime). Thus in this case the fixed point  $\bar{x}_B(s) \equiv 0$  is indeed the saddle point with only one unstable eigenmode  $u_0(s)$  and constitutes the transition state of the chain dynamics bridging the two stable configurations. Since the state  $\bar{x}_B(s) \equiv 0$  corresponds to a compact (coiled) chain conformation at the barrier top and the single unstable mode  $u_0(s) \equiv 1$  represents uniform translation in the  $x$  direction of the whole chain, we conclude that in the parameter regime given by Eq. (14) (except when  $\omega_B^2 \approx K \pi^2 / N^2$ , where a large fluctuation will occur), the chain crosses the barrier in a compact, coiled form.

#### A. The crossing rate below the coil-to-stretch transition

Let us calculate  $\mathcal{R}$  in this coiled-state barrier crossing regime. The net barrier height  $\Delta \Phi$  is the difference between the energies of the two stationary states  $\bar{x}_B$  and  $\bar{x}_0$ :

$$\Delta \Phi = \Phi[\bar{x}_B] - \Phi[\bar{x}_0] = N U_B. \quad (15)$$

The partition functions accounting for the free energies of fluctuation at the well and saddle are calculated from the functional integrations [comparable to the discrete versions Eqs. (5) and (6)],

$$Z_0 = \int_{well} \mathcal{D}[\delta x(s)] e^{-\beta(\Phi[\bar{x}_0 + \delta x] - \Phi[\bar{x}_0])},$$

$$Z_B = \int_{\perp (unstable \ mode)} \mathcal{D}[\delta x(s)] e^{-\beta(\Phi[\bar{x}_B + \delta x] - \Phi[\bar{x}_B])}.$$



For the integrals over fluctuation  $\delta x(s)$ , consider the transformation

$$\delta x(s) = \sum_{j=0}^{N-1} X_j u_j(s) \quad (16)$$

in terms of the eigenfunctions  $u_j(s)$  of the operator  $\Phi$ . Up to second order in  $\delta x$  (harmonic expansion),

$$\Phi[\bar{x} + \delta x] - \Phi[\bar{x}] = \frac{N}{2} \sum_{j=0}^{N-1} \lambda_j X_j^2, \quad (17)$$

with  $\lambda_j$  representing either  $\lambda_j^0$  or  $\lambda_j^B$  (and  $\bar{x}$  representing  $\bar{x}_0$  or  $\bar{x}_B$ ). It turns out that the proper change of integration measure in transforming variables from  $\delta x(s)$  to  $\{X_j\}$  reads

$$\int \mathcal{D}[\delta x(s)] \rightarrow \int d(\sqrt{N}X_0) \cdots d(\sqrt{N}X_{N-1}).$$

Combining these we get, within the harmonic approximation for the variation in  $\Phi$ ,

$$Z_0 = (\sqrt{2\pi k_B T})^N (\lambda_0^0 \cdots \lambda_{N-1}^0)^{-1/2},$$

$$Z_B = (\sqrt{2\pi k_B T})^{N-1} (\lambda_1^B \cdots \lambda_{N-1}^B)^{-1/2},$$

and finally from Eq. (4),

$$\begin{aligned} \mathcal{R} &= \frac{\omega_B}{2\pi\gamma} \frac{(\lambda_0^0 \cdots \lambda_{N-1}^0)^{1/2}}{(\lambda_1^B \cdots \lambda_{N-1}^B)^{1/2}} e^{-\beta N U_B} \\ &= \frac{\omega_B \omega_0}{2\pi\gamma} \prod_{j=1}^{N-1} \frac{\left(\omega_0^2 + \frac{K\pi^2 j^2}{N^2}\right)^{1/2}}{\left(-\omega_B^2 + \frac{K\pi^2 j^2}{N^2}\right)^{1/2}} e^{-\beta N U_B} \\ &\approx \frac{\omega_B \omega_0}{2\pi\gamma} \left(\frac{\omega_B^2}{\omega_0^2}\right)^{1/4} \left(\frac{\sinh(N\sqrt{\omega_0^2/K})}{\sin(N\sqrt{\omega_B^2/K})}\right)^{1/2} e^{-\beta N U_B}, \quad (18) \end{aligned}$$

for  $-\omega_B^2 + (K\pi^2/N^2) > 0$ . The last approximation holds for  $N \gg 1$ . In the strong coupling limit  $K \rightarrow \infty$ , the rate becomes  $\mathcal{R}(K \rightarrow \infty) \rightarrow (\omega_B \omega_0 / 2\pi\gamma) e^{-\beta N U_B} \equiv \mathcal{R}_0$ .  $\mathcal{R}_0$  is the rate expected when the  $N$ -bead chain acts like a single globule, collapsed by infinitely large tension [15]. As the chain attains flexibility by decreasing  $K$ , the rate increases. For all ranges of parameters satisfying the condition  $-\omega_B^2 + (K\pi^2/N^2) > 0$ , the activation energy barrier itself remains the same:  $\Phi[\bar{x}_B] - \Phi[\bar{x}_0] = N U_B$ , and the effect of flexibility is wholly contained in the prefactor of the rate, which represents the effect of chain fluctuation near the saddle and well configurations. For a fixed  $K$ , the rate  $\mathcal{R} = \mathcal{R}(N)$  is also enhanced with increasing  $N$  compared to its globular-chain limit  $\mathcal{R}_0(N)$  by the factor

$$\mathcal{R}/\mathcal{R}_0 = \left(\frac{\omega_B^2}{\omega_0^2}\right)^{1/4} \left(\frac{\sinh(N\sqrt{\omega_0^2/K})}{\sin(N\sqrt{\omega_B^2/K})}\right)^{1/2} > 1, \quad (19)$$

increasing with  $N$ , while  $-\omega_B^2 + (K\pi^2/N^2) > 0$ .

A singular feature of the above rate expression obtained by harmonic approximation of  $\delta\Phi$  is that it diverges as  $\lambda_1^B = -\omega_B^2 + (K\pi^2/N^2)$  goes to zero:  $\mathcal{R}[-\omega_B^2 + (K\pi^2/N^2) \rightarrow 0] \rightarrow \infty$ . We can think of  $(\lambda_1^B)^{1/2}$  as the frequency of the first internal (Rouse) mode of a harmonic chain renormalized at the barrier top with curvature  $\omega_B^2$ ; when the intrinsic mode eigenvalue  $(K\pi^2/N^2)$  matches the external force constant  $\omega_B^2$ ,  $\lambda_1^B$  vanishes to allow infinite fluctuation of the chain. This causes the free energy of the chain at the barrier top to decrease indefinitely, and the rate apparently diverges. This singularity is an artifact of the harmonic approximation where the quartic term of the potential is neglected, i.e., the potential is treated as  $U(x) = -(\omega_B^2/2)x^2$ .

The singularity in  $\mathcal{R}$  can be removed by including higher-order (anharmonic) terms of  $X_j$ 's in calculation of  $Z_B$ . Since the fluctuation along the  $j=0$  mode does not contribute to  $Z_B$ , inserting  $\delta x(s) = \sum_{j=1}^{N-1} X_j u_j(s)$  into  $\delta\Phi_B \equiv \Phi[\bar{x}_B + \delta x] - \Phi[\bar{x}_B] = \Phi[\delta x]$ , we get the relevant anharmonicity correction to  $\delta\Phi_B$ :

$$\delta\Phi_B = \frac{N}{2} \sum_{j=1}^{N-1} \lambda_j^B X_j^2 + \frac{3}{8} N \omega_B^2 \frac{1}{\xi^2} X_1^4. \quad (20)$$

Now with the corrected expression Eq. (20), the barrier partition function becomes

$$\begin{aligned} Z_B &= \int d(\sqrt{N}X_1) e^{-\beta[(N/2)\lambda_1^B X_1^2 + (3/8)N\omega_B^2(1/\xi^2)X_1^4]} \\ &\quad \times \int d(\sqrt{N}X_2) \cdots d(\sqrt{N}X_{N-1}) e^{-\beta(N/2) \sum_{j=2}^{N-1} \lambda_j^B X_j^2} \\ &= (\sqrt{2\pi k_B T})^{N-1} (\lambda_1^B \cdots \lambda_{N-1}^B)^{-1/2} f\left(\frac{\epsilon}{\epsilon^*}\right), \end{aligned}$$

where

$$f(\alpha) = \sqrt{\frac{\alpha}{2\pi}} \int_{-\infty}^{\infty} dQ e^{-(\alpha/2)Q^2 - (3/8)Q^4},$$

$$\epsilon \equiv \lambda_1^B / \omega_B^2 = -1 + \frac{K\pi^2}{\omega_B^2 N^2}, \quad (21)$$

and

$$\epsilon^* \equiv \frac{1}{\xi} \sqrt{\frac{k_B T}{N\omega_B^2}}. \quad (22)$$

The  $\epsilon$  is the fractional difference between the first Rouse mode eigenvalue  $(K\pi^2/N^2)$  and the barrier curvature  $(\omega_B^2)$ , or is proportional to the fractional difference between the polymer kinetic energy and potential energy at the barrier

[15]. In the following we will use  $\epsilon$  as a small parameter describing the coil-to-stretch transition. The  $f(\alpha)$  goes to unity for  $\alpha \gg 1$ , and is proportional to  $\sqrt{\alpha} \propto \sqrt{\lambda_1^B}$  for  $\alpha \ll 1$ . Hence the  $\epsilon^*$  represents the value of  $\epsilon$  below which the anharmonicity correction to the rate becomes important. Since we are considering the case of (total barrier height)  $= (1/4)N\omega_B^2\xi^2 \gg k_B T$  in order for the Kramers rate theory to be valid, we can say  $\epsilon^* \ll 1$ . The above expression of  $Z_B$  has no singularity as  $\lambda_1^B \rightarrow 0$ , and reduces to the result of second-order calculation when  $\epsilon \gg \epsilon^*$ .

The rate now can be written

$$\mathcal{R} = \mathcal{R}_h f\left(\frac{\epsilon}{\epsilon^*}\right), \quad (23)$$

where  $\mathcal{R}_h$  represents the rate expression equation (18) calculated with the harmonic expansion of  $\delta\Phi_B$ .

### B. The crossing rate above the coil-to-stretch transition

Now let us see what happens immediately above the coil-to-stretch transition. Since  $\lambda_1^B$  and  $\epsilon$  tend to be negative, not only the mode  $u_0(s)$  but also  $u_1(s)$  tend to be unstable at the barrier top. This signals the emergence of a new saddle point configuration  $\bar{x}_B(s)$  with smaller energy and only one unstable mode. Indeed, we find a nontrivial solution to Eq. (10) centered at  $x=0$  with the free-end boundary condition. The solution corresponds to a stretched chain configuration traversing the barrier top ( $x=0$ ) only once at  $s=\frac{1}{2}$ . This is analogous to the kink, or one-instanton, solution in  $\phi^4$ -field theory. The  $\epsilon=0$ , therefore, marks the conformational transition that we call coil-to-stretch transition. For small  $|\epsilon| = |\lambda_1^B/\omega_B^2|$ , we can find the solution perturbatively by inserting  $\bar{x}(s) = \bar{x}_B(s) = \sum_{j=1}^{N-1} X_j u_j(s)$  to Eq. (10). By multiplying each side of the resulting equation by  $u_j(s)$  and integrating over  $0 \leq s \leq 1$ , we get coupled equations relating coefficients  $X_1, X_2, \dots, X_{N-1}$ . We find that as  $|\epsilon| = -\epsilon$  grows from zero,  $X_1$  grows as  $X_1 \sim |\epsilon|^{1/2}$ , while all other coefficients scale as  $X_j (j \geq 2) \sim |\epsilon|^{3/2}$  or smaller. Hence for  $|\epsilon| \ll 1$ , we can well approximate the solution  $\bar{x}_B(s)$  by the first cosine mode

$$\bar{x}_B(s) \approx X_1 u_1(s) = X_1 \sqrt{2} \cos(\pi s), \quad (24)$$

$X_1$  being  $X_1 = \xi \sqrt{2|\epsilon|/3}$ .

Now the corresponding activation energy is calculated to be

$$\Delta\Phi = \Phi[\bar{x}_B(s)] - \Phi[\bar{x}_0] = NU_B - \frac{1}{6}N\omega_B^2\xi^2\epsilon^2. \quad (25)$$

This represents the decrease in activation energy due to the chain adaptability to external forcing, that is, the ability of the chain to make conformational transition to an energetically more favorable, stretched state at the barrier. For large  $|\epsilon|$ , we can calculate the saddle point configuration and the activation energy by numerically solving Eq. (10). Figure 2 shows the resulting reduction in activation energy  $\Delta\Phi$  as

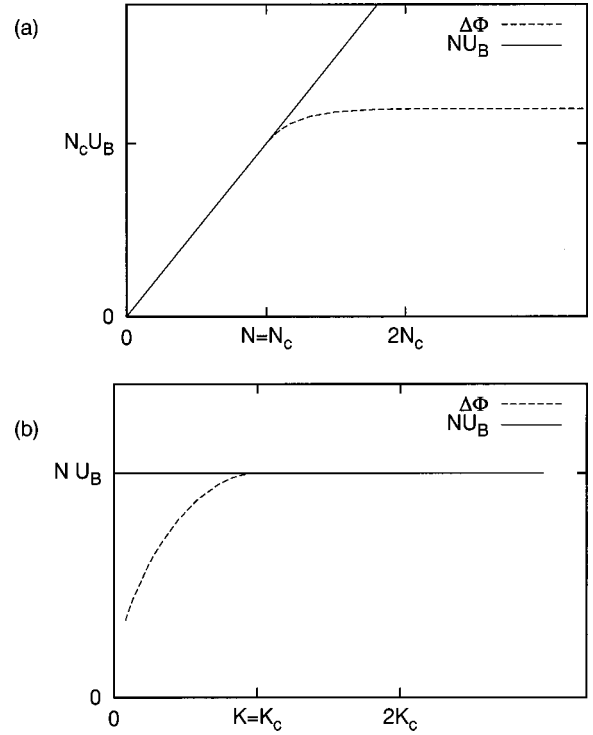


FIG. 2. Activation energy for a harmonic chain surmounting quartic double-well potential barrier. (a)  $\Delta\Phi$  vs  $N$  for fixed tension  $K$  of the harmonic chain.  $N=N_c = \pi\sqrt{K/\omega_B^2}$  corresponds to the coil-to-stretch transition point  $\epsilon=0$ . (b)  $\Delta\Phi$  vs  $K$  for fixed  $N$ .  $K=K_c = \omega_B^2 N^2/\pi^2$  corresponds to the transition point.

functions of  $N$  and  $K$ . Note that the activation energy does not depend on  $N$  at large  $N$  because of deformation (stretching) of the chain over the barrier. A similar effect has been reported in an experiment on long DNA chains with different lengths escaping from entropic trapping [14], and was also mentioned in the recent theoretical work by Sebastian and Paul [16]. The eigenvalue spectrum of normal modes at  $\bar{x}_B(s)$  shows renormalization of the curvature  $\tilde{\omega}_B^2$  along the unstable direction in the reaction path (which, in the previous case of  $\epsilon > 0$ , has been the same as the geometrical curvature  $\omega_B^2$  of the real potential barrier), and the restriction of fluctuation near this point along stable directions. Again we can calculate these eigenvalues perturbatively for small  $|\epsilon|$ . From Eq. (13), the second-order expansion operator at  $\bar{x}_B(s)$  is

$$\Phi \leftrightarrow -\frac{K}{N^2} \frac{d^2}{ds^2} - \omega_B^2 + 4\omega_B^2 |\epsilon| \cos^2(\pi s).$$

The last term is proportional to the small parameter  $|\epsilon|$  and makes a ‘‘perturbation potential’’ in the Schrödinger-type operator  $\Phi$ . By applying the first-order perturbation theory of quantum mechanics,

$$\delta\lambda_j^B = \int_0^1 ds u_j(s)^2 4\omega_B^2 |\epsilon| \cos^2(\pi s) = \begin{cases} 2|\epsilon|\omega_B^2, & j=0 \\ 3|\epsilon|\omega_B^2, & j=1 \\ 2|\epsilon|\omega_B^2, & j \geq 2, \end{cases} \quad (26)$$

we get the normal mode eigenvalues for the (slightly) stretched chain:

$$\begin{aligned}
 (\tilde{\omega}_B)^2 &\equiv |\lambda_0^B| = (1 - 2|\epsilon|)\omega_B^2, & (27) \\
 \lambda_1^B &= -\omega_B^2 + \frac{K\pi^2}{N^2} + 3|\epsilon|\omega_B^2 = -|\epsilon|\omega_B^2 + 3|\epsilon|\omega_B^2 \\
 &= 2|\epsilon|\omega_B^2 > 0, \\
 \lambda_{j \geq 2}^B &= -\omega_B^2 + \frac{K\pi^2 j^2}{N^2} + 2|\epsilon|\omega_B^2.
 \end{aligned}$$

Note that the first ( $j=1$ ) mode is indeed stable, and all the higher modes have larger eigenvalues (representing more restricted fluctuation) about the stretched state  $\bar{x}_B(s)$  of Eq. (24) than they would have about the coiled state  $\bar{x}(s) \equiv 0$ .

Now up to the second-order expansion for  $\delta\Phi_B$  as before,

$$\begin{aligned}
 Z_B &= (\sqrt{2\pi k_B T})^{N-1} \frac{1}{\sqrt{2}} \\
 &\times \prod_{j=1}^{N-1} \left( -\omega_B^2(1-2|\epsilon|) + \frac{K\pi^2 j^2}{N^2} \right)^{-1/2},
 \end{aligned}$$

from which the rate becomes

$$\begin{aligned}
 \mathcal{R}_h &= 2 \frac{\tilde{\omega}_B}{2\pi\gamma} \sqrt{2\pi k_B T} \frac{Z_B}{Z_0} e^{-\beta\Delta\Phi} \\
 &\approx \frac{\tilde{\omega}_B \omega_0}{2\pi\gamma} \sqrt{2} \left( \frac{\tilde{\omega}_B^2}{\omega_0^2} \right)^{1/4} \left( \frac{\sinh(N\sqrt{\omega_0^2/K})}{\sin(N\sqrt{\tilde{\omega}_B^2/K})} \right)^{1/2} \\
 &\times e^{-\beta[NU_B - N\omega_B^2 \xi^2 \epsilon^2/6]}, & (28)
 \end{aligned}$$

$$N \gg 1, \quad \text{for } \epsilon < 0, |\epsilon| \ll 1.$$

The multiplication factor 2 in the first line of the above equation comes from the fact that there are two symmetric transition states (with the same eigenmode structure)  $\bar{x}_B(s)$  and  $\bar{x}_B(1-s)$ .

As in the case  $\epsilon > 0$ , the above  $\mathcal{R}$  diverges at  $\epsilon \rightarrow -0$ , due to infinitely large fluctuation near the state  $\bar{x}_B(s)$  at the conformational transition point of the chain. We can again regularize this by inserting an anharmonic correction term into the partition function  $Z_B$  to get

$$\mathcal{R} = \mathcal{R}_h g\left(\frac{\epsilon}{\epsilon^*}\right), \quad (29)$$

where  $\mathcal{R}_h$  is given by Eq. (28) and the function  $g$  is defined as

$$g(\alpha) = \frac{1}{2} \sqrt{\frac{|\alpha|}{\pi}} e^{-\alpha^2/6} \int_{-\infty}^{\infty} dQ e^{-(\alpha/2)Q^2 - (3/8)Q^4}. \quad (30)$$

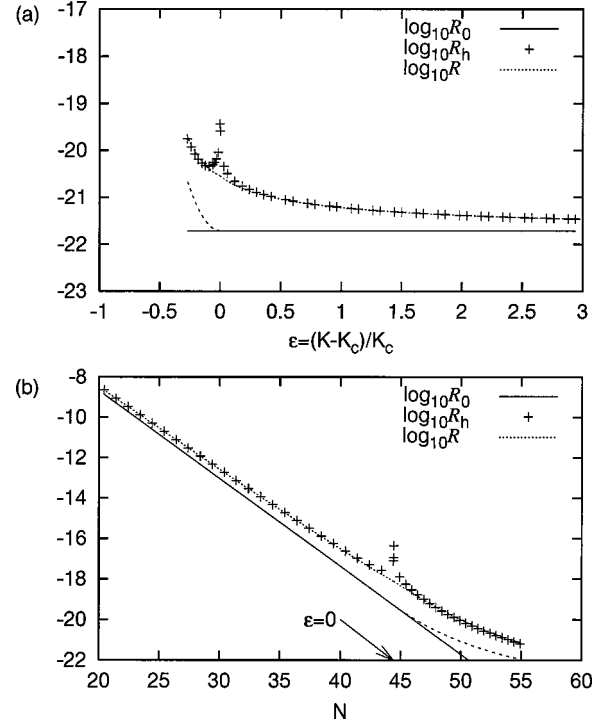


FIG. 3. Rate of barrier crossing of a harmonic chain over a double-well potential barrier. The potential parameters are  $\omega_0^2/\omega_B^2 = 2$ ,  $\beta U_B = 1$ ,  $\xi/\sqrt{k_B T/\omega_B^2} = 2$ . (a) Rate vs  $K$ .  $N=50$ ,  $K_c = \omega_B^2 N^2/\pi^2 = 253\omega_B^2$ . (b) Rate vs  $N$ .  $K$  is fixed at  $K/\omega_B^2 = 200$  for which  $N_c = \pi\sqrt{K/\omega_B^2} = 44.4$ .  $\mathcal{R}_0$  is the rate when the chain crosses the barrier in a globular form.  $\mathcal{R}_h$  is the rate calculated via second-order expansion of  $\delta\Phi$ , while  $\mathcal{R}$  represents the first anharmonicity correction to  $\mathcal{R}_h$ . All the rates are in units of  $\omega_B \omega_0 / (2\pi\gamma)$ . The dashed lines show the Boltzmann factor (in log scale)  $e^{-\beta\Delta\Phi}$  associated with the ‘bare’ activation energy (without fluctuation effect) of the chain.

The rate expressions Eq. (23) and Eq. (29) match continuously and nearly smoothly at  $\epsilon=0$  as shown in Figs. 3(a) and 3(b). Figure 3(a) depicts the rate as a function of  $K$  for fixed  $N=50$  and Fig. 3(b) the rate with varying  $N$  for fixed  $K=200\omega_B^2$ . The stretched-state barrier crossing regime  $\epsilon < 0$  corresponds to either  $K < K_c = \omega_B^2 N^2/\pi^2$  or  $N > N_c = \pi\sqrt{K/\omega_B^2}$ . These figures summarize the rate calculations in this section and suggest some important points worth noting. First, the general trend toward large increase of the rate for  $\epsilon < 0$  (compared to  $\mathcal{R}_0$ ) is due to the drop in activation energy after the conformational transition of the chain to a stretched state. The Boltzmann factor associated with this decreasing  $\Delta\Phi$  is plotted for comparison with dashed lines in both Figs. 3(a) and 3(b). Second, the rate shows remarkable enhancement compared to  $\mathcal{R}_0$  above the enhancement due to the substantial decrease in activation energy. This is because the increased chain fluctuation gives rise to a reduction in the free-energy barrier. Calculations based on the second-order expansion of  $\delta\Phi_B$  overestimate this effect to predict diverging  $\mathcal{R}_h$ . Our regularization scheme by anharmonicity correction seems to be satisfactory in describing the (nearly) smoothly varying rate across the transition point, in good agreement with the numerical simulation shown in Sec. IV.

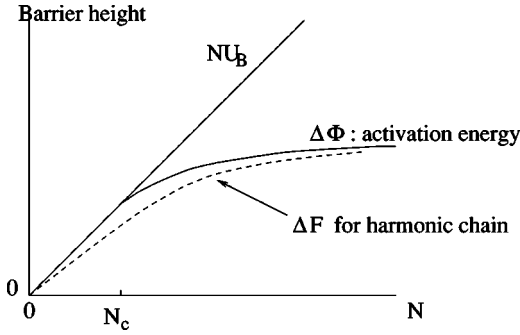


FIG. 4. Schematic plot of the free-energy barrier  $\Delta F$  for a harmonic chain surmounting a double-well potential barrier compared to the activation energy  $\Delta\Phi$ .

*Beyond the Small  $|\epsilon|$  Approximation.* In the above, we have calculated the rate below and just above the coil-to-stretch transition, i.e., the rate for  $\epsilon > 0$  and  $\epsilon < 0$  with  $|\epsilon| \ll 1$ . Evidently, the parameter regime that involves substantial chain extension over the barrier is important and of much relevance in experimental settings. A description of the case with very large  $N$  or very small tension will eventually require theoretical approaches very different from those used here, since we may not be able to identify a localized transition state in the chain configuration space. For moderate  $N$  and tension for which the approach in the preceding sections remains valid, we can in principle always calculate the rate above the coil-to-stretch transition point ( $\epsilon < 0$ ) by numerically solving Eq. (10) for  $\bar{x}_B(s)$  and calculating the eigenvalues of the operator in Eq. (13) [21]. Here we give general analytical predictions on the behavior of  $\mathcal{R}$  when a substantial extension of the chain at the barrier is involved in our model. We discuss in terms of the effective free-energy barrier  $\Delta F$  defined in Eq. (8).

With the model potential  $U(x) = -(\omega_B^2/2)x^2 + \frac{1}{4}(\omega_B^2/\xi^2)x^4$ , the saddle point configuration  $\bar{x}_B(s)$  above the coil-to-stretch transition ( $\epsilon < 0$ ) will be contained in the range  $-\xi < \bar{x}_B(s) < \xi$ . For a harmonic chain, the fluctuation near this configuration is governed by the operator  $\Phi \leftrightarrow U''[\bar{x}_B(s)] - (K/N^2)(d^2/ds^2)$ . Since at any point  $x$  between  $-\xi$  and  $\xi$  the second derivative  $U''(x)$  is smaller than at  $x = -\xi$ ,  $U''(x) < U''(-\xi) = \omega_0^2$ , all the stable (positive) eigenvalues of  $\Phi$  at  $\bar{x}_B(s)$  are smaller than those at the homogeneous configuration  $\bar{x}_0(s) \equiv -\xi$ . That is,

$$\lambda_j^B < \lambda_j^0, \quad j = 1, \dots, N-1.$$

This leads directly to  $Z_B > Z_0'$  or, in view of Eq. (8),  $\Delta F < \Delta\Phi$ . The free-energy barrier is less than the activation energy since the fluctuation is more restricted at the well than at the barrier. This is generally true regardless of the exact shape of the double-well potential  $U(x)$  as long as the chain is harmonic.

Figure 4 shows schematically the expected behavior of  $\Delta F$  (dashed line) with increasing  $N$ . The difference  $\Delta\Phi - \Delta F$  is large near the coil-to-stretch transition point  $\epsilon = 0$ .

The gap may be reduced for larger  $N$  since more segments will be likely to be confined in the well regions, but it remains positive throughout. Note that the rate itself will not show a plateau as the barrier does ( $\Delta\Phi$  or  $\Delta F$ ) for very large  $N$ . This is because the unstable mode frequency  $\tilde{\omega}_B$  is also dependent on  $N$  and goes to zero for large  $N$  (the renormalization of barrier curvature). Eventually, the escape dynamics will show a crossover to the kink diffusion regime where the chain crosses the barrier by diffusive motion of the kink obtained as a solution to Eq. (10). The crossing time in this case was reported to be proportional to  $N^2$  if the potential is symmetric [16].

Our finding that the polymer crosses the barrier by forming a stretched portion (kink) at the barrier top is reminiscent of the kink nucleation in the overdamped soliton theory that has been widely studied in literature (for example, [22]). However, while in the kink nucleation problem one generally considers an infinitely long string (or a string long enough to contain many kinks as localized objects), here we are interested in the case of a relatively short chain for which the barrier crossing process is dominated by the activation of the whole chain on the barrier top, rather than the kink diffusion mechanism. The latter appears when the chain becomes sufficiently long, and our analysis has been focused on the transition between the short and long chain behaviors. We showed that at a critical chain length  $N_c$  or at a critical coupling constant  $K_c$ , the saddle point structure of the problem is modified, which dramatically changes the crossing rate. The fluctuation effect at such a transition point is crucial in determining the rate, and gives a divergent rate if we simply adopt the harmonic approximation scheme as is done in many problems with fixed saddle point structure (including the kink nucleation problem). We identified the regime where the harmonic expansion is insufficient, and calculated the fluctuation effect in that regime by including the leading-order anharmonic term in the expansion of the chain fluctuation [see Eq. (20)].

#### IV. NUMERICAL SIMULATION

Here we report the results of numerical simulation of the barrier crossing dynamics of a harmonic chain under the potential  $U(x) = -(\omega_B^2/2)x^2 + \frac{1}{4}(\omega_B^2/\xi^2)x^4$ . The parameter range covered is not comprehensive, but the simulation supports the general conclusion of the preceding section and confirms the reliability of the analytical methods there. The starting point is the Langevin equation governing the motion of the  $x$  component of the  $n$ th bead [23],

$$\begin{aligned} \gamma \frac{dx_n}{dt} = & \omega_B^2 x_n - \frac{\omega_B^2}{\xi^2} x_n^3 + K(x_{n-1} + x_{n+1} - 2x_n) \\ & + \sqrt{2\gamma k_B T} \xi_n(t), \end{aligned} \quad (31)$$

where  $\gamma$  is the damping constant for one bead and  $\xi_n(t)$  represents the Gaussian white noise satisfying

$$\langle \xi_n(t) \rangle = 0,$$



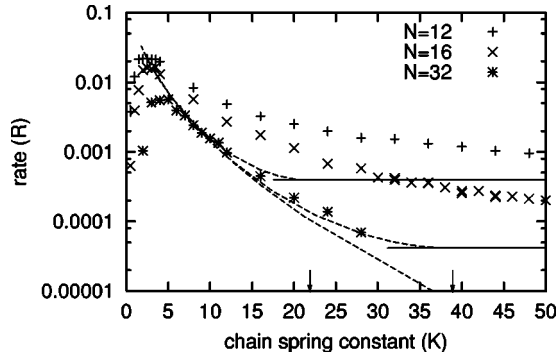


FIG. 5. The simulation result of the rate. Barrier crossing rate (inverse mean time) is plotted against the coupling constant  $K$  of a harmonic chain for  $N=12,16,32$ . The units are chosen such that the barrier curvature  $\omega_B^2=1.5$  (see text). Hence, the unit of measure for  $K$  is  $\omega_B^2/1.5$  and for the rate  $\omega_B/\sqrt{1.5}$ . Horizontal solid lines show the globular limit value  $\mathcal{R}_0$  for  $N=12$  (upper line) and 16 (lower line). Dashed lines are the rates expected from the reduced activation energy  $\Delta\Phi < NU_B$  at  $K < K_c$  for  $N=12,16,32$  (from the top). The arrows indicate  $K_c$  for  $N=12,16$ .

$$\langle \xi_n(t) \xi_m(t') \rangle = \delta_{nm} \delta(t-t'), \quad n, m = 1, 2, \dots, N.$$

We integrate this equation using the Euler-Maruyama method with finite time interval  $\Delta t$  [24]. The random force  $\xi_n(t)$  at each time step is modeled by an independent Gaussian random variable with zero mean and variance  $\sigma^2 = 1/\Delta t$ . The finiteness of time interval is not important when it is much smaller than any macroscopic relaxation time. We require

$$\Delta t \ll \frac{\gamma}{K},$$

where  $\gamma/K$  is the single segment relaxation time, which is the shortest time scale of internal mode relaxation of the chain. The time and length scales of the problem are set by choosing the potential parameters as  $\omega_B^2 = \xi^2 = 1.5$ . We have been assuming unit mass for each bead. In this unit, we choose  $\gamma=1$  and  $k_B T=1$ . (For comparison, the barrier height for a single bead is  $\omega_B^2 \xi^2 / 4 = 0.5625$ .) At  $t=0$ ,  $\{x_n\}$  is in the homogeneous configuration  $x_n = -\xi$  in the left well of the potential  $U(x)$ . Then, for each realization of  $\{x_n(t)\}$  dictated by Eq. (31), we record the time required for the chain to enter the right well, specified by the condition  $x_n(t) > \xi/2$ , for all  $n$ . The inverse of this time averaged over  $M$  ( $\gg 1$ ) realizations is identified as the escape rate  $\mathcal{R}$ .

Figure 5 shows the result for  $N=12,16,32$ , with varying  $K$ . The coil-to-stretch transition point  $K=K_c$  is marked by an arrow for  $N=12$  and 16. The solid lines show the globular limit escape rate  $\mathcal{R}_0$  for  $N=12,16$ .  $\mathcal{R}_0$  for  $N=32$  is too small and beyond the range of the figure. The dashed lines show the rate estimated by taking into account the decrease of the activation energy  $\Delta\Phi$  for  $K < K_c$  (but not the fluctuation effect around the stationary states). The seemingly large discrepancy between these estimates and the simulation results comes from neglecting the fluctuation effect contained

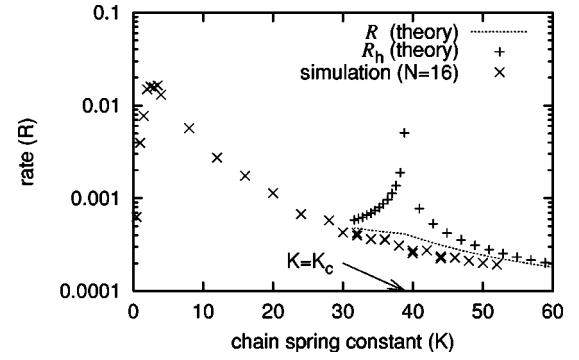


FIG. 6. Same simulation data as in Fig. 5 for  $N=16$  compared to the full analytical result of  $\mathcal{R}$  in Sec. III (dotted line). Rate  $\mathcal{R}_h$  containing the fluctuation effect up to second order fails to give correct results near  $K=K_c$ . Again, the unit of measure for  $K$  is  $\omega_B^2/1.5$  and for the rate  $\omega_B/\sqrt{1.5}$ .

in the prefactor of Eqs. (18) and (28), which in fact is found to enhance the rate by nearly one order of magnitude near  $K=K_c$ .

Figure 6 shows our full analytical results for the rate in Sec. III, in comparison with the simulation data for  $N=16$ . The rate  $\mathcal{R}_h$  obtained by the second-order calculation of the fluctuation integral overestimates the rate near  $K=K_c$  by exaggerating the free-energy decrease at the barrier top due to enhanced fluctuation of the chain. The rate  $\mathcal{R}$  obtained after the leading-order anharmonicity correction to  $\mathcal{R}_h$  shows fairly good agreement with the simulation result and captures reasonably well the gradual increase in the rate with decreasing  $K$  near  $K_c$ .

A remarkable feature of our simulation results is that the rate is *maximized* at a small value of  $K$  for each  $N$ . The rate of such an ‘‘optimized’’ barrier crossing decreases very slowly with increasing  $N$ . In this parameter regime of weak coupling, it is found that interwell dislocation of the whole chain occurs via frequent individual crossing and recrossing of the beads across the barrier. This regime is beyond the scope of analytical calculation of the present work. The turnover of the rate occurs as a result of competition between the coherent motion of the chain (which favors large  $K$ ) and the efficient dynamics achieved by reduced activation energy (which favors small  $K$ ).

## V. SUMMARY

In this paper we have calculated the rate of thermally activated escape of a linear chain out of a local minimum of an external bistable potential. We have identified the escape process as a stochastic process occurring in the chain configuration space and applied multidimensional Kramers rate theory to calculate the rate. Using the continuous model of the chain, we found the stationary points of the chain energy functional and calculated the free energy of fluctuation near these points using the functional integral formalism. The saddle point structure of the chain energy functional plays a crucial role in determining the rate. For large  $N$  ( $N > N_c$ ) or small coupling strength ( $K < K_c$ ), the homogeneous saddle point configuration changes to a ‘‘kink’’ configuration which

corresponds to a stretched chain state at the barrier top. This coil-to-stretch transition greatly lowers the activation energy of the chain, and thus greatly enhances the escape rate of a flexible chain compared to that of a rigid, globular one.

Calculation of the effect of chain fluctuation on the escape rate is an important result of the present study. For a harmonic chain, fluctuation around the stationary configuration is always more favored at the barrier than at the well, due to confinement of the chain at the well. This effect results in an even lower free-energy barrier that the chain must surmount,  $\Delta F < \Delta \Phi$ , and is most prominent near the coil-to-stretch transition point  $N = N_c$  or  $K = K_c$ .

Our calculation in Sec. III shows that above the coil-to-stretch transition, a chain extended over the parabolic barrier range renormalizes the barrier curvature  $\omega_B^2$  to a smaller value. This comes from the extended nature of a stretched chain sensing different points of the potential curve with different curvatures, and leads to effective *slowdown* of chain dynamics at the barrier. This effect will strengthen for a longer chain, and in a symmetric potential, the unstable mode at the saddle point will eventually become a mode with a vanishing eigenvalue. The escape dynamics then follows

the sequential translocation or kink diffusion scheme, of which a relevant description will be in terms of the effective reaction coordinate as in the polymer translocation through a membrane [10], or by direct application of kink nucleation and diffusion theory as in [16].

In summary, conformational change and fluctuation of a flexible chain renormalizes the external barrier to significantly change the escape dynamics quantified by the rate. Identification and calculation of various aspects of this flexibility-induced effect are the main subjects of this paper. Apart from the possibility of direct application to biotechnological processes such as electrophoresis, the present study provides a valuable analytical model that enhances understanding of interesting and relevant features of thermally activated processes of a soft, complex system.

#### ACKNOWLEDGMENTS

We acknowledge support from the Korea Research Foundation (1999) made via POSTECH Institute of Polymer Research.

- 
- [1] *Stochastic Dynamics*, edited by L. Schimansky-Geier and T. Pöschel (Springer, Berlin, 1997).
- [2] P. Hänggi, P. Talkner, and M. Borkovec, *Rev. Mod. Phys.* **62**, 251 (1990); *New Trends in Kramers' Reaction Rate Theory*, edited by P. Talkner and P. Hänggi (Kluwer, Dordrecht, 1995), and references therein.
- [3] R.F. Gröte and J.T. Hynes, *J. Chem. Phys.* **73**, 2715 (1980).
- [4] C.R. Doering and J.C. Gadoua, *Phys. Rev. Lett.* **69**, 2318 (1992); M. Bier and R.D. Astumian, *ibid.* **71**, 1649 (1993).
- [5] H. Grabert, P. Olschowski, and U. Weiss, *Phys. Rev. B* **36**, 1931 (1987).
- [6] J.F. Lindner, B.K. Meadows, W.L. Ditto, M.E. Inchiosa, and A.R. Bulsara, *Phys. Rev. Lett.* **75**, 3 (1995).
- [7] A. Neiman, *Phys. Rev. E* **49**, 3484 (1994).
- [8] A. Ajdari, *J. Phys. I* **11**, 1577 (1994).
- [9] Z. Csahók, F. Family, and T. Vicsek, *Phys. Rev. E* **55**, 5179 (1997).
- [10] P.J. Park and W. Sung, *Phys. Rev. Lett.* **77**, 783 (1996).
- [11] J.J. Kasianowicz, E. Brandin, D. Branton, and P.W. Deamer, *Proc. Natl. Acad. Sci. U.S.A.* **93**, 1377 (1996).
- [12] G.W. Slater, H.L. Guo, and G.I. Nixon, *Phys. Rev. Lett.* **78**, 1170 (1997).
- [13] M. Muthukumar and A. Baumgärtner, *Macromolecules* **29**, 8517 (1996).
- [14] J. Han, S.W. Turner, and H.G. Craighead, *Phys. Rev. Lett.* **83**, 1688 (1999).
- [15] P.J. Park and W. Sung, *J. Chem. Phys.* **111**, 5259 (1999).
- [16] K.L. Sebastian and Alok K.R. Paul, *Phys. Rev. E* **62**, 927 (2000); K.L. Sebastian, *ibid.* **61**, 3245 (2000).
- [17] S. Lee, M.S. thesis, Pohang University of Science and Technology, 1999.
- [18] J.S. Langer, *Ann. Phys. (N.Y.)* **54**, 258 (1969).
- [19] M. Doi and S.F. Edwards, *The Theory of Polymer Dynamics* (Clarendon, Oxford, 1986).
- [20] See, for example, Chap. 3 of E.R. Pinch, *Optimal Control and the Calculus of Variations* (Oxford University Press, Oxford, 1993).
- [21] Direct numerical calculation of the chain free energy at the well and at the barrier top using the transition matrix method has been suggested by Park and Sung [15]. Calculating the chain free energy with its center of mass (COM) fixed at the barrier top, as suggested there, gives a strictly correct barrier partition function when the unstable normal mode is the COM translation mode  $u_0(s)$ . However, for the case where the chain extends over a nonquadratic potential barrier, the unstable mode can be grossly different from  $u_0(s)$ .
- [22] M. Büttiker and R. Landauer, *Phys. Rev. Lett.* **43**, 1453 (1979); *Phys. Rev. A* **23**, 1397 (1981).
- [23] A.Y. Grosberg and A.R. Khokhlov, *Statistical Physics of Macromolecules* (AIP Press, New York, 1994).
- [24] P.E. Kloeden and E. Platen, *Numerical Solution of Stochastic Differential Equations* (Springer-Verlag, Berlin, 1992).